Journal of Experimental Botany, Vol. 65, No. 13, pp. 3769–3779, 2014
doi:10.1093/jxb/eru238
This paper is available online free of all access charges (see http://jxb.oxfordjournals.org/open_access.html for further details)

Journal of Experimental Botany
www.jxb.oxfordjournals.org

RESEARCH PAPER

A high throughput gas exchange screen for determining rates of photorespiration or regulation of C_4 activity

Chandra Bellasio[1,2], Steven J Burgess[2], Howard Griffiths[2] and Julian M Hibberd[2]

[1] Department of Animal and Plant Sciences, University of Sheffield, Western Bank, Sheffield S10 2TN, UK
[2] Department of Plant Sciences, University of Cambridge, Downing Street, Cambridge CB2 3EA, UK

Received 10 April 2014; Revised 1 May 2014; Accepted 1 May 2014

Abstract

Large-scale research programmes seeking to characterize the C_4 pathway have a requirement for a simple, high throughput screen that quantifies photorespiratory activity in C_3 and C_4 model systems. At present, approaches rely on model-fitting to assimilatory responses (A/C_i curves, PSII quantum yield) or real-time carbon isotope discrimination, which are complicated and time-consuming. Here we present a method, and the associated theory, to determine the effectiveness of the C_4 carboxylation, carbon concentration mechanism (CCM) by assessing the responsiveness of V_O/V_C, the ratio of RuBisCO oxygenase to carboxylase activity, upon transfer to low O_2. This determination compares concurrent gas exchange and pulse-modulated chlorophyll fluorescence under ambient and low O_2, using widely available equipment. Run time for the procedure can take as little as 6 minutes if plants are pre-adapted. The responsiveness of V_O/V_C is derived for typical C_3 (tobacco, rice, wheat) and C_4 (maize, *Miscanthus*, cleome) plants, and compared with full C_3 and C_4 model systems. We also undertake sensitivity analyses to determine the impact of R_{LIGHT} (respiration in the light) and the effectiveness of the light saturating pulse used by fluorescence systems. The results show that the method can readily resolve variations in photorespiratory activity between C_3 and C_4 plants and could be used to rapidly screen large numbers of mutants or transformants in high throughput studies.

Key words: C_4, C_3, photosynthesis, RuBisCO, oxygenation, carboxylation, carbon concentration mechanism (CCM), *Cleome gynandra*, rice, maize, wheat, *Miscanthus*.

Introduction

In most photosynthetic organisms Ribulose Bisphosphate Carboxylase Oxygenase (RuBisCO) catalyses the first key step in carbon assimilation, reacting ribulose-1,5-bisphosphate with CO_2 to produce two molecules of 3-phosphoglycerate (PGA). Oxygen competitively inhibits this reaction and leads to the synthesis of the 2-carbon compound phosphoglycollate, which is recycled to PGA (consuming ATP, and then NADPH) and CO_2 by the photorespiratory cycle (Yoshimura *et al.*, 2004; Sage *et al.*, 2012). The result of photorespiration is a noticeable carbon loss and a consequent metabolic cost for carbon recapture and for the recycling of photorespiratory intermediates (Ehleringer and Pearcy, 1983; Pearcy and Ehleringer, 1984; Eckardt, 2005). Many plants have evolved strategies to reduce photorespiration by increasing the level of CO_2 around RuBisCO, including both crassulacean acid metabolism (CAM) and the C_4 photosynthetic pathway (Dodd *et al.*, 2002; Sage, 2004; Sage *et al.*, 2011; Osborne and Sack, 2012; Griffiths *et al.*, 2013; Owen and Griffiths, 2013). C_4 photosynthesis is most often based on a two-celled carbon concentrating mechanism, where HCO_3^- is first fixed into the four-carbon compound oxaloacetic acid (OAA) in the mesophyll by phospho*enol*pyruvate carboxylase (PEPC). OAA is then reduced to malate or transaminated to aspartate and the resulting C_4-(amino)acid is shuttled into the bundle sheath (BS), where it is decarboxylated, releasing CO_2 for refixation by RuBisCO (Hibberd and Covshoff, 2010; Bellasio and Griffiths, 2014c).

Although the enzymes catalysing the core C_4 carbon concentration mechanism (CCM) are well characterized (Kanai and Edwards, 1999), many of the genes responsible for the

accompanying anatomical alterations or for generating and maintaining expression of the C_4 cycle genes (Hibberd *et al.*, 2008; Langdale, 2011) have yet to be identified. One approach that is increasingly proving useful to identify candidate genes underlying the C_4 pathway is comparative transcriptomics of samples either undergoing C_3 or C_4 photosynthesis (Bräutigam *et al.*, 2011; Gowik *et al.*, 2011; John *et al.*, 2014), or tissues in the process of inducing the full C_4 system (Li *et al.*, 2010; Pick *et al.*, 2011; Chang *et al.*, 2012; Wang *et al.*, 2013). Because stable transformation of C_4 species is typically time-consuming, introduction of RNA interference constructs via a transient *Agrobacterium tumefaciens*-based system would be very helpful in screening these candidates being generated from transcriptomics.

At present, techniques used to screen for mutants possessing defective, or enhanced CCM characteristics are time-consuming (Table 1). Analysing the response of assimilation (A) to decreasing CO_2 concentration in the substomatal cavity (C_i), as A/C_i curves (Long and Bernacchi, 2003; Yin *et al.*, 2011a) can take 45 minutes per replicate leaf, and an appropriate model, which may require *a priori* knowledge of species-specific limitations (Laisk and Edwards, 2000; von Caemmerer, 2000, 2013; Yin and Struik, 2009; Yin *et al.*, 2009; Yin *et al.*, 2011b). $^{13}C/^{12}C$ discrimination during photosynthesis (Evans *et al.*, 1986) can also be used, and a comparison with stomatal conductance allows the internal mesophyll conductance, or extent of CCM or PEPC activity, to be resolved (Meyer *et al.*, 2008; Kromdijk *et al.*, 2010; Pengelly *et al.*, 2010; Bellasio and Griffiths, 2014a, b, c). However, this latter technique is sensitive, and requires either off-line sample preparation for mass spectrometric analyses or specialized laser equipment which is not readily available (Table 1).

In this paper we describe a novel method, and present the associated theory, to determine rates of photorespiration from instantaneous rates of RuBisCO carboxylation and oxygenation. The approach compares concurrent gas exchange and pulse-modulated chlorophyll fluorescence measurements under ambient and low O_2. Under these non-photorespiratory conditions assimilation (A) increases, because RuBisCO competitive inhibition from O_2 is reduced. In contrast, $Y(II)$ decreases because the demand for NADPH associated with photorespiratory by-product cycling (and reduction) is lower, and cannot entirely be offset by the increase in A. The new method combines developments in approaches using gas exchange (Sharkey, 1988; Long and Bernacchi, 2003; Ripley *et al.*, 2007) and the quantitative interpretation of quantum yield (Yin *et al.*, 2004, 2009, 2011b; Yin and Struik, 2009, 2012; Bellasio and Griffiths, 2014b). This new method can be performed with off-the-shelf commercial equipment, which is generally available in ecophysiology laboratories. The

Table 1. *Comparison between methods screening for activity of a functional CCM*

Method	Advantages and limitations	Reference
Dry matter isotopic discrimination	*Specialized equipment *Integrates the isotopic signal throughout growth *Cannot resolve transient changes in assimilatory physiology	Cernusak *et al*. (2013)
On line isotopic discrimination	*Laser is no longer commercially available *Maintenance costs of isotope ratio mass spectrometer *Need of highly skilled operator *Difficult computation and parameterization	Evans *et al.* (1986); Bellasio and Griffiths (2014b); von Caemmerer *et al*. (2014)
A/C_i curves	*Requires *a priori* knowledge of the limitations underpinning each part for the A/C_i curve for correct model fitting *Result may depend on experimental routine	Long and Bernacchi (2003); Yin *et al.* (2009)
Gas exchange and fluorescence	*Requires initial response curve for parameterisation *Requires model fitting	Long and Bernacchi (2003); Martins *et al.* (2013)
O_2 sensitivity of carboxylation efficiency	*Delicate experimental routine	Laisk *et al.* (2002); Yin *et al.* (2009)
Assimilation increase under low O_2	*Ease of determination *Ignores the effect of changing O_2 concentration on $Y(II)$	Sharkey (1988); Ripley *et al.* (2007)
Gas exchange and fluorescence	*Rapid (6 minutes) *Widely available equipment *Independent of leaf size *Ease of determination and calculation *Does not require fitting or parameterisation *Assessment under growth conditions	This study

procedure takes as little as 6 minutes to perform if plants are pre-adapted, making it significantly faster than A/C_i curves and potentially useful as a high-throughput approach for assessing C_4 activity in mutant screens, the progeny from C_3–C_4 crosses or C_3–C_4 intermediates.

Materials and methods

Plants

Plants of *Miscanthus* (*Miscanthus giganteus*), cleome (*Cleome gynandra*), maize (*Zea mays* L.), wheat (*Triticum aestivum* L.), tobacco (*Nicotiana tabacum* L.), and rice (*Oryza sativa* L.) were grown at the Plant Growth Facility located at the University of Cambridge Botanic Garden in controlled environment growth rooms (Conviron Ltd, Winnipeg, Canada) set at 16 h day length, temperature of 25 °C/23 °C (day/night), 40% relative humidity, and photosynthetic photon flux density (PPFD)=300 µmol m^{-2} s^{-1}. Plants were manually watered daily, with particular care to avoid overwatering.

Gas exchange measurements with concurrent PSII yield

Measurements were performed with an infra-red gas analyser (IRGA, a LI6400XT, LI-cor, USA), fitted with a 6400–40 leaf chamber fluorometer. The IRGA was fed with CO_2 (through the IRGA gas mixing unit) and ambient air. Gas flow was set at 150 µmol s^{-1}. Reference CO_2 was set at 200 µmol mol^{-1} (Figure 1 and Table 1) or set alternatively at 400, 300, 200, 150, 100, and 50 µmol s^{-1} (Figure 3). Block temperature was controlled at 35 °C. The fluorometer was set to multiphase pulse with factory setting, target intensity=10 and ramp depth=40% (Loriaux *et al.*, 2013). A portion of a light-adapted leaf was clamped in the cuvette. The leaf was allowed to reach stable photosynthetic conditions under PPFD=300 µmol m^{-2} s^{-1} (factory setting: 90% red, 10% blue). Photosynthesis was measured every 10 s for 30 s (the three values were then averaged) and a multiphase pulse was applied for the determination of *Y(II)*. A humidified 2% O_2/N_2 gas (pre-mixed, BOC, Guilford, UK) was switched to supply the inlet of the IRGA. The gas was allowed to completely flush the cuvette (c. 6 min). Photosynthesis was measured every 10 s for 30 s (the three values were then averaged) and a multiphase pulse was applied for the determination of *Y(II)*. Light was turned off, the inlet was fed with ambient air, the reference CO_2 was set at 500 µmol mol^{-1}, similar to the lab CO_2 concentration (c. 550 µmol mol^{-1}) to minimize the errors caused by CO_2 leakage (Boesgaard *et al.*, 2013), and flow was set to 40 µmol s^{-1}. Once the cuvette had been flushed, and the signal stabilised (c. 5 min), respiration was measured every 10 s for 2 min (the values were then averaged). C_a was not adjusted to account for changes in stomatal conductance or for the control of C_i during this procedure. This avoided the need for IRGA recalibration as the *Y(II)* measurements are independent of C_i. The measured A and *Y(II)* under low and ambient O_2, together with an estimate of R_{LIGHT} (see below), were used to determine RuBisCO rate of carboxylation (V_C), RuBisCO rate of oxygenation (V_O), and the rate of photorespiratory CO_2 evolution in the light (F).

Theory

RuBisCO catalyses two reactions: a carboxylase reaction whereby Ribulose BisPhosphate (RuBP) is carboxylated to form two molecules of phosphoglyceric acid (PGA), and an oxygenase reaction whereby RuBP is oxygenated to form one PGA and one glycollate molecule. Each carboxylase event requires 2 NADPH for the reduction of the 2 PGA molecules formed. Each oxygenase event requires 1 NADPH for the reduction of the PGA directly produced by RuBisCO, 0.5 NADPH to recycle glycollate, and 0.5 NADPH to reduce the PGA regenerated, which total 2 NADPH (Bellasio and Griffiths, 2014c). The overall NADPH demand, at steady-state, equals the total photosynthetic NADPH production rate J_{NADPH} (Yin *et al.*, 2004; Yin and Struik, 2012):

$$J_{NADPH} = 2V_C + 2V_O \tag{1}$$

Where J_{NADPH} is the total NADPH produced for photosynthesis, V_C is RuBisCO carboxylation rate, and V_O is RuBisCO oxygenation rate. Notably, this reducing power requirement is the same for all types of photosynthesis, as active types of CCM require additional ATP but not NADPH. In line with von Caemmerer (2000) equation 1 assumes that PGA is entirely reduced, and therefore the small quantity of PGA consumed by respiration ($\frac{1}{3}R_{LIGHT}$) is neglected, in fact under growth light irradiance $2V_C+2V_O >> \frac{1}{3}R_{LIGHT}$, unless at very low irradiances, see equation 7 in Bellasio and Griffiths (2014c).

Although the carboxylation reaction of RuBisCO consumes CO_2, the regeneration of glycollate releases 0.5 CO_2 for each oxygenase catalytic event. CO_2 is also produced by light respiration, a process which is active during photosynthesis to support basal metabolism. The net assimilation rate (A, which is the quantity measured through gas exchange) results from summing the CO_2 consumed by RuBisCO, the CO_2 produced by glycollate regeneration and the CO_2 produced by respiration:

$$A = V_C - \frac{1}{2}V_O - R_{LIGHT} \tag{2}$$

Where A is net CO_2 assimilation, R_{LIGHT} is respiration in the light and other variables were previously defined. Notably, this equation is universal for all types of photosynthesis (von Caemmerer, 2013).

For the definition of gross assimilation ($GA = A + R_{LIGHT}$), equation 2 can be rearranged:

$$V_C = GA + \frac{1}{2}V_O \tag{3}$$

Equation 1 and 3 can be combined to give:

$$V_O = \frac{J_{NADPH} - 2GA}{3} \tag{4}$$

The rate of photorespiratory CO_2 evolution, F can be calculated as: (von Caemmerer, 2013)

$$F = \frac{1}{2}V_O \tag{5}$$

Under low O_2, V_O can be approximated to ≈0, hence, from equation 4:

$$J_{NADPH\ Low\ O2} = 2GA_{Low\ O2} \tag{6}$$

Which is valid when $V_O \approx 0$.

NADPH is produced through linear electron flow. Independently from where this reaction is located (e.g. in mesophyll cells), electrons are invariably extracted from water by PSII (Yin and Struik, 2012), therefore J_{NADPH} is proportional to *Y(II)* (Yin and Struik, 2012). This allows J_{NADPH} to be calculated under photorespiratory conditions using the information derived under non-photorespiratory conditions, and can be expressed as (Bellasio and Griffiths, 2014b):

$$J_{NADPH} = J_{NADPH\ Low\ O2}\frac{Y(II)}{Y(II)_{Low\ O2}} \tag{7}$$

Where J_{NADPH} and *Y(II)* refer to ambient O_2 conditions. Equation 7 has been validated in C_3 and C_4 plants (Yin *et al.*, 2009, 2011b; Bellasio and Griffiths, 2014b, c) but it is worth noting that equation 7 is a mathematical simplification and holds true when: (i) photorespiration is negligible under non-photorespiratory conditions, which

is a widely used simplification; (ii) R_{LIGHT} does not vary between low and ambient O_2—this is also a fair assumption because any O_2 effect is generally negligible (Badger, 1985; Gupta *et al.*, 2009); (iii) the allocation to alternative sinks (non-assimilatory and non-photorespiratory) is proportional to $Y(II)$. This is the normal case in C_4 plants where the relationship between $Y(II)$ and $Y(CO_2)$ has a null intercept (Edwards and Baker, 1993). When that is not the case, for instance when the allocation to alternative sinks is constant, equation 7 would also hold true if the allocation to alternative sinks is small compared with $Y(II)$. This is the normal case in C_3 plants (Valentini *et al.*, 1995; Martins *et al.*, 2013). Should the allocation to alternative sinks be large, equation 7 would still hold true mathematically when $\frac{Y(II)}{Y(II)_{\text{Low O2}}}$ is close to the unity. The implications for method accuracy are detailed in the discussion.

Equation 3, 4, 6, and 7 can be combined to obtain:

$$\frac{V_O}{V_C} = \frac{2GA_{\text{Low O2}} \frac{Y(II)}{Y(II)_{\text{Low O2}}} - 2GA}{GA_{\text{Low O2}} \frac{Y(II)}{Y(II)_{\text{Low O2}}} + 2GA} \quad (8)$$

Which expresses the RuBisCO rate of oxygenation relative to carboxylation. The influence on the quality of R_{LIGHT} estimate on V_O/V_C is described in the discussion, together with the other factors influencing the results.

Modelling C_3 and C_4 V_O/V_C

The data obtained for tobacco and maize were compared with a simulated V_O/V_C based on the validated von Caemmerer models for C_3 and C_4 photosynthesis. Briefly, for tobacco, the response of A to C_i was modelled using the quadratic equation (Table 3, equation 9) proposed by Ethier and Livingston (2004), which takes into account mesophyll conductance to CO_2. The CO_2 concentration at the site of carboxylation C_C was then calculated through the supply function of mesophyll (equation 10), and, finally V_O/V_C was simulated from the kinetic properties of RuBisCO and the ratio between C_C and the O_2 concentration at the site of carboxylation (equation 11). For maize (Table 4), firstly we simulated the responses of V_P and A to decreasing C_i, using the equations for the enzyme-limited model for C_4 photosynthesis (equation 12 and 16, respectively). These were used to simulate the CO_2 and O_2 concentration in the bundle sheath (equation 13 and 14, respectively), the ratio of which, together with RuBisCO specificity, was used to simulate V_O/V_C (equation 15 and 17).

Results

Figure 1 displays a typical primary data profile for a C_3 tobacco leaf, showing the interaction between steady state assimilation (A) and quantum yield of PSII, $Y(II)$, during the transition from ambient to low O_2 (21 to 2% O_2), with hatched areas indicating the steady state conditions under which readings were taken to derive V_O/V_C. Under non-photorespiratory conditions, A increases because of the lower competitive inhibition of O_2, whereas $Y(II)$ decreases owing to the lower NADPH demand for photorespiratory by-product recycling and reduction. The experimental conditions were deliberately chosen to minimize reductions of quantum yield at saturating light (relatively low PPFD of 300 μmol m^{-2} s^{-1}), and enhance photorespiratory responses to low O_2 partial pressure (measurements at 200 μmol mol^{-1} CO_2) (Fig. 1 and Table 2). Subsequently, V_O/V_C was

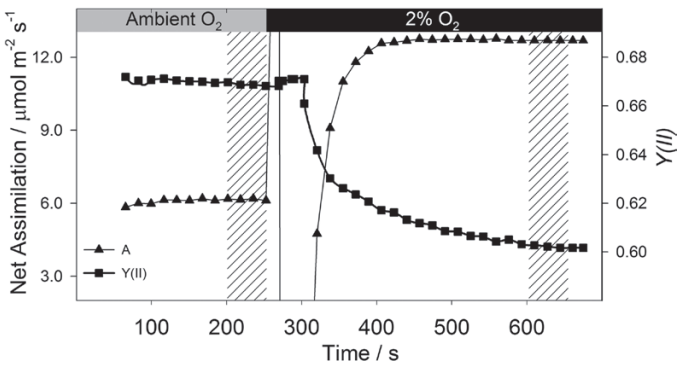

Fig. 1. Summary of experimental approach. One representative dataset from C_3 tobacco is presented. Once stable assimilatory conditions are reached, a first set of data are recorded (left hatched area). The background gas is then switched from ambient to 2% O_2. After a suitable acclimation time to allow flushing of the cuvette and reacclimation (c. 6 min), a second set of data are recorded (right hatched area). The response of assimilation (triangles) and Photosystem II yield $Y(II)$ (squares) during the experiment are shown.

measured on C_3 tobacco and C_4 maize using different CO_2 concentrations in the reference gas: 400, 300, 200, 150, 100, and 50 μmol mol^{-1} (Fig. 2) and results were compared with simulated values of V_O/V_C generated with the validated von Caemmerer C_3 and C_4 models. To facilitate the comparison, data were plotted against the substomatal CO_2 concentration C_i. As expected, under decreasing C_i, V_O/V_C becomes progressively higher in tobacco but it is only marginally affected in maize. The measured data track the trend and magnitude of the theoretical curves in C_3, whereas we could not capture the theoretical increase in V_O/V_C expected when C_i was close to zero. This may be due to errors in the determination of C_i at very low stomatal conductance or to the simplifications used to resolve equation 7. Our data slightly underestimate V_O/V_C derived using pulsed of ^{13}C enriched CO_2 (Busch *et al.*, 2013), which, however, lay above the curve simulated with the von Caemmerer C_3 model (see Fig. 2).

Additional measurements were undertaken with the IRGA, including a recalibration procedure to account for the changing sensitivity to water vapour pressure after the transition to low O_2, but stomatal conductance was reduced on average by 1% and internal CO_2 concentration, C_i, by 3 μmol mol^{-1} (data not shown). In the subsequent sections, primary data for V_O/V_C determinations using this new method (calculated from equation 4) are initially presented for three representatives of C_3 and C_4 species. We then undertake a systematic error analysis of the method, to include the impact of biological and environmental variables. These include physiological components (R_{LIGHT}) and Fm', as well as light intensity and CO_2 concentration used during experimentation.

Variability between and within populations

Table 2 demonstrates that the method clearly discriminates between C_4 species, possessing a functional CCM, and C_3 species with higher rates of photorespiration. V_O/V_C ranged from 0.0435 to 0.0852 for the representative C_4 species, with

Table 2. *Example of variability within populations and between populations displayed by plants with different pathways of assimilation*

V_O/V_C was measured on species (*Miscanthus*, *Cleome gynandra*, maize, wheat, tobacco, and rice) under photosynthetic photon flux density (PPFD) of 300 μmol m^{-2} s^{-1}, and C_a=200 μmol mol^{-1}.

Population	*n*	Mean V_O/V_C	Standard deviation	Coefficient of variation
Miscanthus	7	0.0504	0.0091	18%
Cleome gynandra	5	0.0852	0.0046	5.4%
Maize	4	0.0435	0.0074	17%
Wheat	3	0.522	0.071	14%
Tobacco	4	0.533	0.030	5.5%
Rice	4	0.569	0.037	6.5%

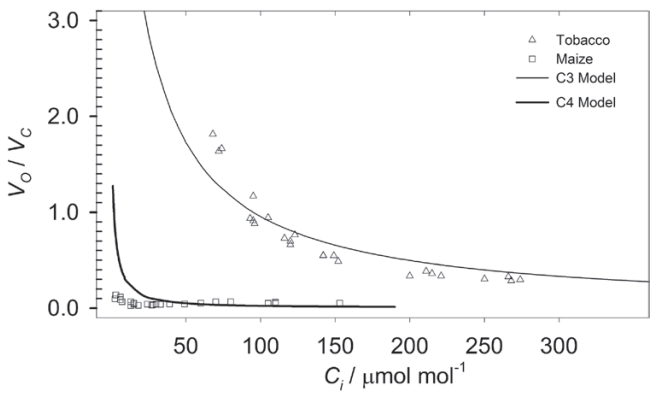

Fig. 2. V_O/V_C measured under different CO_2 concentrations in the substomatal cavity (C_i), obtained by imposing reference CO_2 concentrations of 400, 300, 200, 150, 100, and 50 µmol mol^{-1} for C_3 tobacco (triangles) and C_4 maize (squares). Data are compared with simulated V_O/V_C using the validated von Caemmerer C_3 and C_4 models (lines, see also Table 3 and 4). With decreasing C_i, V_O/V_C gets progressively higher in tobacco but it is only marginally affected in maize, CO_2 concentration can therefore be used to control the resolution of the method. All data shown, *n*=4.

coefficients of variation ranging from c. 15% down to 5% in *C. gynandra* (Table 2). For the C_3 species, V_O/V_C ranged from 0.522 to 0.569, with a low coefficient of variation in tobacco and rice around 6% (Table 2). The magnitude of the offset between C_3 and C_4 systems, if being used as a rapid screen, would allow changes in expression of C_4 characteristics to be clearly resolved. Such an approach would then allow more detailed characterisation of selected transformants, C_2, or C_3–C_4 intermediates to be undertaken.

Accuracy of R_{LIGHT} *estimates*

To account for the extent that R_{LIGHT} affected the measurement of V_O/V_C, a sensitivity analysis was used to determine how R_{LIGHT} influences V_O/V_C (Fig. 3). To do so, equation 8 was calculated for a realistic dataset (R_{LIGHT}=1 µmol m^{-2} s^{-1}, V_O/V_C=0.2 and $Y(II)$=0.65) at variable assimilation values. Then, test values for V_O/V_C were calculated after R_{LIGHT} was varied to 2 µmol m^{-2} s^{-1} (+100%), 1.5 µmol m^{-2} s^{-1} (+50%), 1.2 µmol m^{-2} s^{-1} (+20%), 0.8 µmol m^{-2} s^{-1} (–20%), 0.5 µmol m^{-2} s^{-1} (–50%), 0 µmol m^{-2} s^{-1} (–100%, $GA=A$). The deviation from the set V_O/V_C value (0.2) represented the effect of errors in the evaluation of R_{LIGHT} on V_O/V_C. Figure 3 shows that V_O/V_C was relatively insensitive to R_{LIGHT}: for assimilation rates higher than 4 µmol m^{-2} s^{-1}, R_{LIGHT} values which differed ± 50% resulted in an error lower than 4% in relative terms. R_{LIGHT} overestimation resulted in a lower error than R_{LIGHT} underestimation. For these reasons there is generally no need for a high quality estimate of R_{LIGHT}.

Accuracy of Fm′ *measurements*

Equations 7 and 8 require the photochemical yield of PSII, $Y(II)$. This is determined according to the formula of Genty (Genty *et al.*, 1989; Maxwell and Johnson, 2000; Kramer *et al.*, 2004), whereby $Y(II)$ is calculated as the difference between the light-saturated chlorophyll fluorescence signal (Fm') minus the chlorophyll fluorescence signal measured during photosynthesis (Fs), expressed as relative to Fm'. Key to this technique is achieving full saturation of PSII in the determination of Fm' (Earl and Ennahli, 2004; Loriaux *et al.*, 2006; Harbinson, 2013; Loriaux *et al.*, 2013). Sub-saturating light pulses result in the underestimation of Fm'; however, the degree of underestimation depends not only on the saturating pulse spectra and intensity, but also on the species, the growth light intensity, and the light intensity used during the measurements (Earl and Ennahli, 2004).

Here, we show how a given Fm' underestimation influences the values for V_O/V_C (Fig. 4). To do so, equation 8 was set to physiologically realistic conditions (R_{LIGHT}=1 µmol m^{-2} s^{-1}, V_O/V_C=0.2, and A=5 µmol m^{-2} s^{-1}), at different $Y(II)$ values. Underestimates of Fm' were then introduced by multiplying the realistic Fm' value by, successively, 0.99 (–1%), 0.98 (–2%), 0.97 (–3%), and 0.95 (–5%). The difference between the two values represented the effect of Fm' underestimation on V_O/V_C. Figure 4 shows that V_O/V_C was sensitive to Fm' underestimation; for instance the relative error of V_O/V_C was c. 20% when $Y(II)$ was 0.15 and Fm' was underestimated by 3%. The error increased hyperbolically at decreasing $Y(II)$, and increased proportionally as the Fm' underestimation was increased.

Light intensity and CO_2 *concentration used for experimentation*

High light intensities (e.g. PPFD>1000 µmol m^{-2} s^{-1}) result in a low PSII yield, which may potentially amplify the systematic error from any Fm' underestimation (see above). Similarly, small $Y(II)$ could potentially lead to V_O/V_C underestimation when the allocation to alternative sinks is significant (see description

of equation 7). Further, high light conditions require longer timescales to reach stable photosynthetic conditions. On the other hand, depending on growth conditions, low light intensities (e.g. <100 μmol m^{-2} s^{-1}) might lead to low assimilation rates, which could amplify the systematic errors in the estimation of R_{LIGHT} (see Fig. 3 and above). For these reasons, intermediate light intensities represent the best solution, whereby *Y(II)* and *A* are both high. For instance, values at the top end of the linear region of the *light* response curve would be ideal. These generally correspond to the growth light intensity.

CO_2 concentration in the cuvette (C_a) can be used to manipulate photorespiration. Figure 2 shows the measured and predicted V_O/V_C of C_3 and C_4 plants under different CO_2 concentrations. Because of the CCM, V_O/V_C is low in maize, even at low C_i, whereas in wheat V_O/V_C increases hyperbolically at decreasing C_i. This contrasting behaviour allows the resolution of the method to be manipulated by changing the CO_2 concentration in the background gas. However, decreasing CO_2 concentration is disadvantageous because: (i) low C_i results in quenching of PSII yield, which may potentially amplify the systematic error determined by *Fm′* underestimation (see above); at the same time (ii) low *Y(II)* would amplify the magnitude of V_O/V_C underestimation owing to the partitioning of *Y(II)* to alternative sinks (see description of equation 7); (iii) under low C_a, more time is required to reach stable photosynthetic conditions, which result in lower throughput; (iv) low C_a increases the driving force for diffusion from outside of the cuvette, which may constitute a potential source of error, especially when assimilation is low (Boesgaard *et al.*, 2013). For these reasons the optimal C_a will depend on the purpose of the analysis, and on the desired resolution and speed.

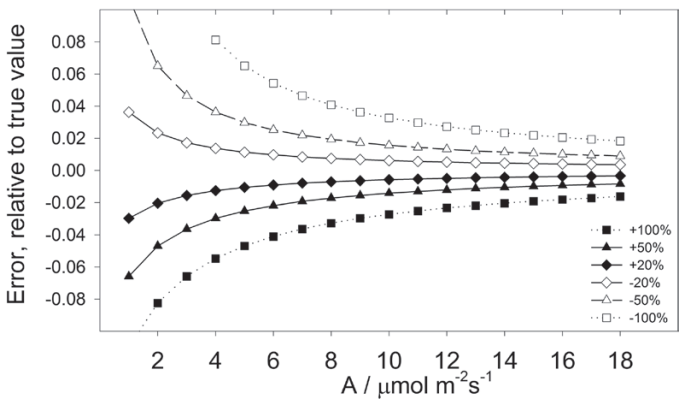

Fig. 3. Sensitivity to errors in the determination of R_{LIGHT}. True values were simulated by calculating equation 8 for R_{LIGHT}=1 μmol m^{-2} s^{-1}, V_O/V_C = 0.2, and *Y(II)*=0.65 at variable assimilation (*A*) values. Test values of V_O/V_C were then calculated by solving equation 8 at different values for R_{LIGHT}: 2 μmol m^{-2} s^{-1} (+100%), 1.5 μmol m^{-2} s^{-1} (+50%), 1.2 μmol m^{-2} s^{-1} (+20%), 0.8 μmol m^{-2} s^{-1} (–20%), 0.5 μmol m^{-2} s^{-1} (–50%), 0 μmol m^{-2} s^{-1} (–100%, *GA*=*A*). The difference in V_O/V_C between the test minus the true value was expressed as relative to the true value.

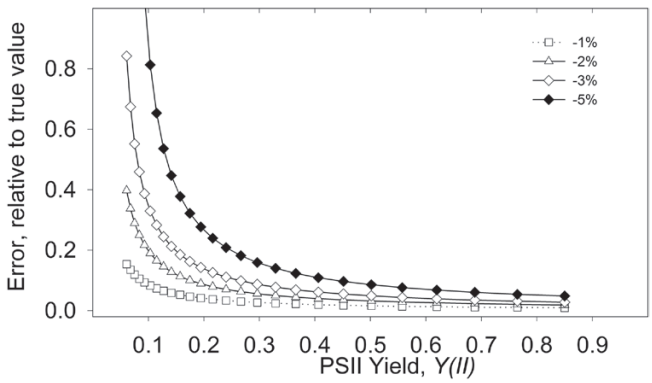

Fig. 4. Sensitivity to errors in the determination of *Fm′*. True values were simulated by calculating equation 8 for R_{LIGHT}=1 μmol m^{-2} s^{-1}, V_O/V_C=0.2 and *A*=5 μmol m^{-2} s^{-1} at different *Y(II)* values. Test values of V_O/V_C were then calculated by solving equation 8 introducing increasing *Fm′* underestimation: –1, –2, –3, and –5%. The difference in V_O/V_C between the test minus the true value was expressed as relative to the true value.

Discussion

This method is based upon the difference in net assimilation (*A*) and photosystem II yield (*Y(II)*) observed when the gas supplied to an actively photosynthesizing leaf is switched from ambient O_2 to low O_2. The goal was to develop a relatively quick, readily available method, which could be used to screen large numbers of transformants, C_3–C_4, C_2, or photorespiratory refixation variants (Busch et al 2013; Oakley *et al.*, 2014) in a given population of plants. The data show that the method readily distinguishes between V_O/V_C for typical C_3 and C_4 plants (Table 2), and, given the low coefficients of variation, should detect more subtle variations in C_4 repression or activation within a screen. It would then be possible to subject plants identified in this way to a more detailed, conventional gas exchange or stable isotope screen, to identify contributory morphological, metabolic or genetic factors. In the subsequent discussion, we explore the theoretical and practical limitations underpinning the accuracy of the method, and improvements that could be instituted to enhance the outputs, if high sample throughput was not a primary limitation.

Other methods have been proposed to determine the contribution of photorespiration *in vivo* through gas exchange measurements. The method proposed by Ripley *et al.* (2007) uses only the increase in assimilation under non-photorespiratory conditions, and therefore ignores the effect on *Y(II)*. In our work we observed that *Y(II)* is generally influenced by changes in O_2 concentration (Figure 1), even in C_4 plants (see Fig. 2 in Bellasio and Griffiths, 2014b); therefore it is important to take into account the feedback from assimilation on photosystem II yield. Long and Bernacchi (Long and Bernacchi, 2003) proposed a comprehensive method to determine the partitioning of total electron transport rate between photorespiratory and assimilatory demand. Their protocol requires an initial light or A/C_i response so as to fit a linear relationship between quantum yield for CO_2 fixation $Y(CO_2)$ and quantum yield of photosystem II, *Y(II)*.

In comparison, the simple method that we have proposed requires no previous parameterization, no curve fitting, and no knowledge of the underpinning physiology or biochemical constants. It is also independent of leaf area, as when

deriving V_O/V_C from equation 8, both the numerator and the denominator are proportional to leaf area, a huge advantage for small or dissected leaves. The likelihood of triose phosphate limitation (Sharkey, 1988) is minimized under the relatively low light intensities and low C_i, which are optimal for this protocol. The determination of V_O/V_C could take as little as c. 6 min, although the complete routine was longer (c. 40 min) as leaves were allowed to acclimate before measurement of both assimilation and dark respiration. Therefore, the run time can be minimized by measuring assimilation under growth conditions (e.g. at growth light intensity and CO_2 concentration), and either measuring respiration after all plants have been collectively dark–adapted, or estimating it separately (see below).

Other factors affecting accuracy of V_O/V_C determination

As shown in Fig. 3, the estimation of R_{LIGHT} is important when calculating gross assimilation using eqn. 8 ($GA=A+R_{LIGHT}$) at low assimilation rates. R_{LIGHT} can be determined with several methods; for instance, by linear regression of assimilation (A) versus irradiance (under very low irradiance e.g. <150 μmol photons m^{-2} s^{-1}), by linear regression of A versus irradiance multiplied by $Y(II)$ [under moderate irradiance, e.g. <400 μmol photons m^{-2} s^{-1} (Yin *et al.*, 2011a)], by non-linear regression [throughout the light response curve (Prioul and Chartier, 1977; Dougherty *et al.*, 1994)] or assumed to equal dark respiration [e.g. (Kromdijk *et al.*, 2010; Ubierna *et al.*, 2013)]. These methods do not necessarily yield the same R_{LIGHT} values, and so, the degree of similarity between different R_{LIGHT} estimates depends on the species and growth conditions. For instance, in Cocklebur (*Xanthium strumarium* L., Asteraceae), R_{LIGHT} was significantly different from dark respiration (Tcherkez *et al.*, 2008), whereas in maize R_{LIGHT} is generally non-significantly different from dark respiration (C. Bellasio, unpublished data). The most suitable method to estimate R_{LIGHT} should therefore be evaluated on a case-by-case basis (see Bellasio and Griffiths, 2014a), and for a uniform population (e.g. one species or set of transformants in a growth chamber), R_{LIGHT} could be estimated on a subset of individuals, with one of the methods described above. If dark respiration is used as a proxy, the quality of the estimate can be increased using large chambers and low flow rates. In a diverse population, R_{LIGHT} could be estimated by measuring

Table 3. *Model for C_3 photosynthesis*

Symbol	Definition/calculation	Equation	Values/Units/References
A	Net Assimilation $A=\frac{-b+\sqrt{b^2-4ac}}{2a}$ where: $a=-\frac{1}{g_m}$; $b=\frac{(V_{Cmax}-R_{LIGHT})}{g_m}+C_i+K_C(1+\frac{O}{K_O})$; $c=R_{LIGHT}\left(C_i+K_C(1+\frac{O}{K_O})\right)-V_{Cmax}\left(C_i-\Gamma^*\right)$	(9)	Ethier and Livingston (2004)
C_c	CO_2 partial pressure at the site of carboxylation $C_c=C_i-\frac{A}{g_m}$	(10)	μbar
C_i	CO_2 concentration in the intercellular spaces as calculated by the IRGA.		μmol mol^{-1} (Li-cor 6400 manual equation 1–18)
g_m	Mesophyll conductance to CO_2		0.25 mol m^{-2} s^{-1} bar^{-1} (Ethier and Livingston, 2004)
K_C	RuBisCO Michaelis-Menten constant for CO_2		319.3 μbar (Ethier and Livingston, 2004)
K_O	RuBisCO Michaelis-Menten constant for O_2		277 100 μbar (Ethier and Livingston, 2004)
O	O_2 partial pressure at the site of carboxylation		200 000 μbar
R_{LIGHT}	Respiration in the light		0.63 μmol m^{-2} s^{-1}
V_{Cmax}	Maximum RuBisCO carboxylation rate		34.7 μmol m^{-2} s^{-1} (Ethier and Livingston, 2004)
V_O/V_C	$\frac{V_O}{V_C}=\frac{V_{Omax}K_C}{V_{Cmax}K_O}\frac{O}{C_C}$	(11)	equation 2.16 in (von Caemmerer, 2000)
V_{Omax}	Maximum RuBisCO oxygenation rate		13.25 μmol m^{-2} s^{-1} (Ethier and Livingston, 2004)
Γ^*	CO_2 compensation point in absence of dark respiration		44 μbar

Table 4. *Model for C_4 photosynthesis*

Symbol	Definition/calculation	Equation	Values/Units/References
A	Net Assimilation $A=\frac{-b-\sqrt{b^2-4ac}}{2a}$ where: $a=1-\frac{\alpha K_C}{0.047K_O}$; $b=-\left\{(V_P-R_M+g_{BS}C_M)+(V_{Cmax}-R_{LIGHT})+g_{BS}K_C\left(1+\frac{O_M}{K_O}\right)+\frac{\alpha}{0.047}(\gamma^* V_{Cmax}+R_{LIGHT}\frac{K_C}{K_O})\right\}$; $c=(V_{Cmax}-R_{LIGHT})(V_P-R_M+g_{BS}C_M)-(V_{Cmax}g_{BS}\gamma^* O_M+R_{LIGHT}g_{BS}K_C\left(1+\frac{O_M}{K_O}\right))$	(12)	Equation 4.21 in (von Caemmerer, 2000)
C_{BS}	CO_2 concentration in the bundle sheath $C_{BS}=\frac{\gamma^* O_{BS}+K_C\left(1+\frac{O_{BS}}{K_O}\right)\frac{A+R_{LIGHT}}{V_{Cmax}}}{1-\frac{A+R_{LIGHT}}{V_{Cmax}}}$	(13)	Equation 4.11 in (von Caemmerer, 2000)
C_M	CO_2 partial pressure in M (at the site of PEP carboxylation) $C_M = C_i$		µbar
C_i	CO_2 concentration in the intercellular spaces as calculated by the IRGA		µbar
g_{BS}	Bundle sheath conductance to CO_2		0.005 mol m^2 s^{-1}
K_C	RuBisCO Michaelis-Menten constant for CO_2		650 µbar (von Caemmerer, 2000)
K_O	RuBisCO Michaelis-Menten constant for O_2		450 000 µbar (von Caemmerer, 2000)
K_P	PEPC Michaelis-Menten constant		80 µbar (von Caemmerer, 2000)
O_{BS}	O_2 mol fraction in the bundle sheath cells (in air at equilibrium) $O_{BS}=O_M+\frac{\alpha A}{0.047g_{BS}}$	(14)	µmol mol^{-1} Equation 4.16 in (von Caemmerer, 2000)
O_M	O_2 partial pressure in the mesophyll cells (in air at equilibrium)		210 000 µbar
R_{LIGHT}	Respiration in the light, assumed to equal dark respiration		
R_M	Mesophyll non photorespiratory CO_2 production in the light $R_M = 0.5\ R_{LIGHT}$		µmol m^{-2} s^{-1} (von Caemmerer, 2000; Kromdijk *et al.*, 2010; Ubierna *et al.*, 2013)
V_{Cmax}	Maximum RuBisCO carboxylation rate		60 µmol m^{-2} s^{-1} (von Caemmerer, 2000
V_O/V_C	$\frac{V_O}{V_C}=\frac{2\Gamma^*}{C_{BS}}$	(15)	Equation 4.8 in (von Caemmerer, 2000)
V_P	PEP Carboxylation rate $V_P=\frac{C_M V_{Pmax}}{C_M+K_P}$	(16)	Equation 4.17 in (von Caemmerer, 2000)
V_{Pmax}	Maximum PEPC carboxylation rate		120 µmol m^{-2} s^{-1} (von Caemmerer, 2000)
α	Fraction of PSII active in BS cells		0.15 (Edwards and Baker, 1993; von Caemmerer, 2000; Kromdijk *et al.*, 2010)
γ^*	Half of the reciprocal of the RuBisCO specificity		0.000193 (von Caemmerer, 2000)
Γ^*	CO_2 compensation point in absence of dark respiration $\Gamma^* = \gamma^* O_{BS}$	(17)	Equation 4.9 in (von Caemmerer, 2000)

dark respiration on each individual plant after the measurements in the light.

As shown in Fig. 3, errors in the determination of *Fm′* suggest that techniques such as the multiphase flash (Loriaux *et al.*, 2013), or initial checks to ensure that the saturating pulse is saturating (see Bellasio and Griffiths, 2014b) are normally appropriate for this method. However, the use of our method is possible without a multiphase flash. Firstly, the underestimation of *Fm′* introduces a systematic error, i.e. comparable plants will normally show similar V_O/V_C (see Bellasio *et al.*, 2014), unless the extent of C_4 or C_2 activity has changed under these conditions. Thus, the precision and the resolution of the method, when comparing different phenotypes against a common genetic background, are not affected by a consistent underestimation of *Fm′*. Secondly, to improve accuracy, i.e. the capacity of the method to estimate the true V_O/V_C, other approaches could: (i) increase the saturating pulse intensity; (ii) reduce the distance between light source or fibre-optic probe and leaf (in some systems); (iii) decrease actinic light intensity (as shown in this study) to maximise *Y(II)*; and (iv) CO_2 concentration can be increased, in order to maximise *Y(II)*.

IRGA recalibration, matching Y(II), C_i, *and consideration of mesophyll conductance*

As mentioned in the results, a slight effect on stomatal conductance and C_i (under low O_2) could have been caused by not recalibrating the IRGA upon switching background gas (Bunce, 2002). Although that recalibration could have increased C_i and g_S accuracy (under low O_2), this procedure

is liable to introduce operator error and extend the time taken for measurements; further, there are theoretical reasons why we need not account for these processes while carrying out such a simple comparative screen. Firstly, the data used to calculate equation 8 are measured by the CO_2 channel of the IRGA and the fluorometer, which are both unaffected by the background gas (Bunce, 2002). Secondly, the effect of C_i on A (under low O_2) is, for the greatest part, accounted by the feedback on $Y(II)$. Although C_i decreases under low O_2, there is a strong feedback between assimilation and $Y(II)$, and therefore $Y(II)$ decreases proportionally. In fact, the relationship between gross assimilation (or, better, between $Y(CO_2)$, which is GA divided by PPFD) and $Y(II)$ is strictly linear (Edwards and Baker, 1993; Valentini *et al.*, 1995; Martins *et al.*, 2013). In C_4 plants, this linear relationship has generally a zero intercept, (Edwards and Baker, 1993); therefore, for C_4 plants, there is no need for curve fitting and the relationship can be correctly estimated with a single point. In C_3 systems this relationship is still linear but the intercept is, although generally small, not zero. The intercept, which is the magnitude of engagemant of alternative sinks, can be estimated by linear curve fitting, although several data points are required (Valentini *et al.*, 1995; Martins *et al.*, 2013). Using the complete fitting of the $Y(CO_2)/Y(II)$ relationship, however, did not improve the estimate of V_O/V_C (data not shown): the complete curve fitting correctly estimates the intercept, but the datapoints are taken under conditions which differ from those under which V_O/V_C is measured.

Another way to improve the estimate of V_O/V_C would be to adjust C_a under low O_2 so as to match $Y(II)$ measured under ambient O_2 with $Y(II)$ measured under low O_2. Alternatively, C_a could be manipulated to deliver C_i under low O_2, which matches that under ambient. The advantages would be that the measured data would then probably fit the predicted C_3 and C_4 models more precisely when C_i is limiting (see Fig. 2, Tables 3 and 4). However, these operations do not improve the capacity to screen between C_3 and C_4 photosynthesis and the additional manipulations increase time and likelihood of errors. We also note that such improvements would allow this method to be used to calculate the CO_2 concentration at the site of carboxylation (C_C) in C_3 plants through equation 11 (Table 3), as well as mesophyll conductance via equation 10, using C_C, and the values for assimilation and C_i measured under ambient conditions.

Conclusion

In this paper a simple method, and associated theory, have been presented, which allow the determination of both the oxygenation (V_O) and carboxylation (V_C) rate of RuBisCO and the rate of photorespiratory CO_2 evolution (F) based on gas exchange and variable chlorophyll fluorescence under ambient and low O_2. This may be of particular interest for high throughput screening to identify C_4 mutants lacking a fully functional CCM, C_2 variants, or populations of C_3–C_4 hybrids (Oakley *et al.*, 2014).

Acknowledgments

We thank Shu-Yi Yang, Ross Dennis, Chris John for plants, as well as EU FP7 Marie Curie ITN Harvest, grant no. 238017, the Cambridge Philosophical Society (HG and CB), and the BBSRC (JMH and SJB) for funding. The authors have no conflict of interest.

References

Badger MR. 1985. Photosynthetic oxygen exchange. *Annual Review of Plant Physiology* **36,** 27–53.

Bellasio C, Fini A, Ferrini F. 2014. Evaluation of a high throughput starch analysis optimised for wood. *Plos ONE* **9,** e86645.

Bellasio C, Griffiths H. 2014*a*. Acclimation of C_4 metabolism to low light in mature maize leaves could limit energetic losses during progressive shading in a crop canopy. *Journal of Experimental Botany* **65,** 3725–3736.

Bellasio C, Griffiths H. 2014*b*. Acclimation to low light by C_4 maize: Implications for bundle sheath leakiness. *Plant Cell and Environment* **37,** 1046–1058.

Bellasio C, Griffiths H. 2014*c*. The operation of two decarboxylases (NADPME and PEPCK), transamination and partitioning of C_4 metabolic processes between mesophyll and bundle sheath cells allows light capture to be balanced for the maize C_4 pathway. *Plant Physiology* **164,** 466–480.

Boesgaard KS, Mikkelsen TN, Ro-Poulsen H, Ibrom A. 2013. Reduction of molecular gas diffusion through gaskets in leaf gas exchange cuvettes by leaf-mediated pores. *Plant, Cell and Environment* **36,** 1352–1362.

Bräutigam A, Kajala K, Wullenweber J *et al*. 2011. An mRNA blueprint for C_4 photosynthesis derived from comparative transcriptomics of closely related C_3 and C_4 species. *Plant Physiology* **155,** 142–156.

Bunce J. 2002. Sensitivity of infrared water vapor analyzers to oxygen concentration and errors in stomatal conductance. *Photosynthesis Research* **71,** 273–276.

Busch FA, Sage TL, Cousins AB, Sage RF. 2013. C_3 plants enhance rates of photosynthesis by reassimilating photorespired and respired CO_2. *Plant, Cell and Environment* **36,** 200–212.

Cernusak LA, Ubierna N, Winter K, Holtum JAM, Marshall JD, Farquhar GD. 2013. Environmental and physiological determinants of carbon isotope discrimination in terrestrial plants. *New Phytologist* **200,** 950–965.

Chang Y-M, Liu W-Y, Shih AC-C, Shen M-N, Lu C-H, Lu M-YJ, Yang H-W, Wang T-Y, Chen SC-C, Chen SM. 2012. Characterizing regulatory and functional differentiation between maize mesophyll and bundle sheath cells by transcriptomic analysis. *Plant Physiology* **160,** 165–177.

Dodd AN, Borland AM, Haslam RP, Griffiths H, Maxwell K. 2002. Crassulacean acid metabolism: plastic, fantastic. *Journal of Experimental Botany* **53,** 569–580.

Dougherty RL, Bradford JA, Coyne PI, Sims PL. 1994. Applying an empirical model of stomatal conductance to three C_4 grasses. *Agricultural and Forest Meteorology* **67,** 269–290.

Earl H, Ennahli S. 2004. Estimating photosynthetic electron transport via chlorophyll fluorometry without Photosystem II light saturation. *Photosynthesis Research* **82,** 177–186.

Eckardt NA. 2005. Photorespiration revisited. *The Plant Cell* **17,** 2139–2141.

Edwards GE, Baker NR. 1993. Can CO_2 assimilation in maize leaves be predicted accurately from chlorophyll fluorescence analysis. *Photosynthesis Research* **37,** 89–102.

Ehleringer J, Pearcy RW. 1983. Variation in quantum yield for CO_2 uptake among C_3 and C_4 plants. *Plant Physiology* **73,** 555–559.

Ethier GJ, Livingston NJ. 2004. On the need to incorporate sensitivity to CO_2 transfer conductance into the Farquhar-von Caemmerer-Berry leaf photosynthesis model. *Plant, Cell and Environment* **27,** 137–153.

Evans JR, Sharkey TD, Berry JA, Farquhar GD. 1986. Carbon isotope discrimination measured concurrently with gas-exchange to investigate CO_2 diffusion in leaves of higher plants. *Australian Journal of Plant Physiology* **13,** 281–292.

Genty B, Briantais JM, Baker NR. 1989. The relationship between the quantum yield of photosynthetic electron-transport and quenching of chlorophyll fluorescence. *Biochimica et Biophysica Acta* **990,** 87–92.

Gowik U, Bräutigam A, Weber KL, Weber APM, Westhoff P. 2011. Evolution of C_4 photosynthesis in the genus *Flaveria*: How many and which genes does it take to make C_4? *The Plant Cell Online* **23,** 2087–2105.

Griffiths H, Weller G, Toy LFM, Dennis RJ. 2013. You're so vein: bundle sheath physiology, phylogeny and evolution in C_3 and C_4 plants. *Plant, Cell and Environment* **36,** 249–261.

Gupta KJ, Zabalza A, Van Dongen JT. 2009. Regulation of respiration when the oxygen availability changes. *Physiologia Plantarum* **137,** 383–391.

Harbinson J. 2013. Improving the accuracy of chlorophyll fluorescence measurements. *Plant, Cell and Environment* **36,** 1751–1754.

Hibberd JM, Covshoff S. 2010. The regulation of gene expression required for C_4 photosynthesis. *Annual Review of Plant Biology* **61,** 181–207.

Hibberd JM, Sheehy JE, Langdale JA. 2008. Using C_4 photosynthesis to increase the yield of rice—rationale and feasibility. *Current Opinion in Plant Biology* **11,** 228–231.

John CR, Smith-Unna RD, Woodfield H, Hibberd JM. 2014. Evolutionary convergence of cell specific gene expression in independent lineages of C_4 grasses. *Plant Physiology* doi: 10. 1104/pp.114.238667.

Kanai R, Edwards GE. 1999. The biochemistry of C_4 photosynthesis. In: Sage RF, Monson RK, eds. *C4 plant biology*. San Diego: Academic Press, 49–88.

Kramer D, Johnson G, Kiirats O, Edwards G. 2004. New fluorescence parameters for the determination of QA redox state and excitation energy fluxes. *Photosynthesis Research* **79,** 209–218.

Kromdijk J, Griffiths H, Schepers HE. 2010. Can the progressive increase of C_4 bundle sheath leakiness at low PFD be explained by incomplete suppression of photorespiration? *Plant, Cell and Environment* **33,** 1935–1948.

Laisk A, Edwards GE. 2000. A mathematical model of C4 photosynthesis: The mechanism of concentrating CO2 in NADP-malic enzyme type species. *Photosynthesis Research* **66**, 199–224.

Laisk A, Oja V, Rasulov B, Ramma H, Eichelmann H, Kasparova I, Pettai H, Padu E, Vapaavuori E. 2002. A computer-operated routine of gas exchange and optical measurements to diagnose photosynthetic apparatus in leaves. *Plant, Cell and Environment* **25,** 923–943.

Langdale JA. 2011. C_4 cycles: Past, present, and future research on C_4 photosynthesis. *The Plant Cell Online* **23,** 3879–3892.

Li P, Ponnala L, Gandotra N, Wang L, Si Y, Tausta SL, Kebrom TH, Provart N, Patel R, Myers CR. 2010. The developmental dynamics of the maize leaf transcriptome. *Nature Genetics* **42,** 1060–1067.

Long SP, Bernacchi CJ. 2003. Gas exchange measurements, what can they tell us about the underlying limitations to photosynthesis? Procedures and sources of error. *Journal of Experimental Botany* **54,** 2393–2401.

Loriaux S, Burns R, Welles J, McDermitt D, Genty B. 2006. Determination of maximal chlorophyll fluorescence using a multiphase single flash of sub-saturating intensity. *American Society of Plant Biologists Annual Meeting*. Boston, MA.

Loriaux SD, Avenson TJ, Welles JM, McDermitt DK, Eckles RD, Riensche B, Genty B. 2013. Closing in on maximum yield of chlorophyll fluorescence using a single multiphase flash of sub-saturating intensity. *Plant, Cell and Environment* **36,** 1755–1770.

Martins SCV, Galmés J, Molins A, DaMatta FM. 2013. Improving the estimation of mesophyll conductance to CO_2: on the role of electron transport rate correction and respiration. *Journal of Experimental Botany* **64,** 3285–3298.

Maxwell K, Johnson GN. 2000. Chlorophyll fluorescence—a practical guide. *Journal of Experimental Botany* **51,** 659–668.

Meyer M, Seibt U, Griffiths H. 2008. To concentrate or ventilate? Carbon acquisition, isotope discrimination and physiological ecology of early land plant life forms. *Philosophical Transactions of the Royal Society B: Biological Sciences* **363,** 2767–2778.

Oakley JC, Sultmanis S, Stinson CR, Sage TL, Sage RF. 2014. Comparative studies of C_3 and C_4 *Atriplex* hybrids in the genomics era: physiological assessments. *Journal of Experimental Botany* **7,** 3637–3647.

Osborne CP, Sack L. 2012. Evolution of C_4 plants: a new hypothesis for an interaction of CO_2 and water relations mediated by plant hydraulics. *Philosophical Transactions of the Royal Society B-Biological Sciences* **367,** 583–600.

Owen NA, Griffiths H. 2013. A system dynamics model integrating physiology and biochemical regulation predicts extent of crassulacean acid metabolism (CAM) phases. *New Phytologist* **200,** 1116–1131.

Pearcy RW, Ehleringer J. 1984. Comparative ecophysiology of C_3 and C_4 plants. *Plant, Cell and Environment* **7,** 1–13.

Pengelly JJL, Sirault XRR, Tazoe Y, Evans JR, Furbank RT, von Caemmerer S. 2010. Growth of the C_4 dicot *Flaveria bidentis*: photosynthetic acclimation to low light through shifts in leaf anatomy and biochemistry. *Journal of Experimental Botany* **61,** 4109–4122.

Pick TR, Brautigam A, Schluter U *et al*. 2011. Systems analysis of a maize leaf developmental gradient redefines the current C_4 model and provides candidates for regulation. *Plant Cell* **23,** 4208–4220.

Prioul JL, Chartier P. 1977. Partitioning of transfer and carboxylation components of intracellular resistance to photosynthetic CO_2 fixation: A critical analysis of the methods used. *Annals of Botany* **41,** 789–800.

Ripley BS, Gilbert ME, Ibrahim DG, Osborne CP. 2007. Drought constraints on C_4 photosynthesis: stomatal and metabolic limitations in C_3 and C_4 subspecies of *Alloteropsis semialata*. *Journal of Experimental Botany* **58,** 1351–1363.

Sage RF. 2004. The evolution of C_4 photosynthesis. *New Phytologist* **161,** 341–370.

Sage RF, Christin P-A, Edwards EJ. 2011. The C_4 plant lineages of planet Earth. *Journal of Experimental Botany* **62,** 3155–3169.

Sage RF, Sage TL, Kocacinar F. 2012. Photorespiration and the evolution of C_4 photosynthesis. *Annual Review of Plant Biology* **63,** 19–47.

Sharkey TD. 1988. Estimating the rate of photorespiration in leaves. *Physiologia Plantarum* **73,** 147–152.

Tcherkez G, Bligny R, Gout E, Mahé A, Hodges M, Cornic G. 2008. Respiratory metabolism of illuminated leaves depends on CO_2 and O_2 conditions. *Proceedings of the National Academy of Sciences, USA* **105,** 797–802.

Ubierna N, Sun W, Kramer DM, Cousins AB. 2013. The efficiency Of C_4 photosynthesis under low light conditions in *Zea Mays*, *Miscanthus* × *Giganteus* and *Flaveria Bidentis*. *Plant, Cell and Environment* **36,** 365–381.

Valentini R, Epron D, De Angelis P, Matteucci G, Dreyer E. 1995. *In situ* estimation of net CO_2 assimilation, photosynthetic electron flow and photorespiration in Turkey oak (*Q. cerris* L.) leaves: diurnal cycles under different levels of water supply. *Plant, Cell and Environment* **18,** 631–640.

von Caemmerer S. 2000. *Biochemical models of leaf Photosynthesis*. Collingwood: CSIRO Publishing.

von Caemmerer S. 2013. Steady-state models of photosynthesis. *Plant, Cell and Environment* **36,** 1617–1630.

von Caemmerer S, Ghannoum O, Pengelly JJL, Cousins AB. 2014. Carbon isotope discrimination as a tool to explore C4 photosynthesis. *Journal of Experimental Botany*.

Wang P, Kelly S, Fouracre JP, Langdale JA. 2013. Genome-wide transcript analysis of early maize leaf development reveals gene cohorts associated with the differentiation of C_4 Kranz anatomy. *The Plant Journal* **75,** 656–670.

Yin X, Struik PC. 2009. C_3 and C_4 photosynthesis models: An overview from the perspective of crop modelling. *Njas-Wageningen Journal of Life Sciences* **57,** 27–38.

Yin X, Struik PC, Romero P, Harbinson J, Evers JB, Van Der Putten PEL, Vos JAN. 2009. Using combined measurements of gas exchange and chlorophyll fluorescence to estimate parameters of a biochemical C_3 photosynthesis model: a critical appraisal and a new integrated approach applied to leaves in a wheat (*Triticum aestivum*) canopy. *Plant, Cell and Environment* **32,** 448–464.

Yin X, Sun Z, Struik PC, Gu J. 2011*a*. Evaluating a new method to estimate the rate of leaf respiration in the light by analysis of combined gas exchange and chlorophyll fluorescence measurements. *Journal of Experimental Botany* **62,** 3489–3499.

Yin X, Van Oijen M, Schapendonk A. 2004. Extension of a biochemical model for the generalized stoichiometry of electron transport limited C_3 photosynthesis. *Plant, Cell and Environment* **27,** 1211–1222.

Yin XY, Struik PC. 2012. Mathematical review of the energy transduction stoichiometries of C_4 leaf photosynthesis under limiting light. *Plant, Cell and Environment* **35,** 1299–1312.

Yin XY, Sun ZP, Struik PC, Van der Putten PEL, Van Ieperen W, Harbinson J. 2011*b*. Using a biochemical C_4 photosynthesis model and combined gas exchange and chlorophyll fluorescence measurements to estimate bundle-sheath conductance of maize leaves differing in age and nitrogen content. *Plant, Cell and Environment* **34,** 2183–2199.

Yoshimura Y, Kubota F, Ueno O. 2004. Structural and biochemical bases of photorespiration in C_4 plants: quantification of organelles and glycine decarboxylase. *Planta* **220,** 307–317.